Pathways for dissociative methane chemisorption on Pt{110}-(1×2)

A. T. Anghel, D. J. Wales, S. J. Jenkins, and D. A. King
Department of Chemistry, University of Cambridge, Lensfield Road, Cambridge CB2 1EW, United Kingdom
(Received 20 December 2004; published 24 March 2005; corrected 10 May 2005)

Two distinct pathways are characterized for dissociative chemisorption of methane on Pt{110}-(1×2). The transition states are obtained to high precision using a fully unconstrained technique involving hybrid eigenvector-following with variational eigenvector refinement and tangent space minimization. The two paths yield products where methyl occupies a ridge atop site, with the dissociated hydrogen in one of two distinct ridge bridge sites. Both pathways involve simultaneous stretching of a C—H bond and deformation of methane bond angles, in agreement with experimentally observed rate enhancement.

DOI: 10.1103/PhysRevB.71.113410 PACS number(s): 68.43.Bc, 68.47.De, 71.15.Mb

The conversion of low value natural gas to higher value petrochemicals is of tremendous industrial importance. The mechanism of CH_4 dissociation on single metal surfaces has therefore attracted considerable attention.[1–8] However, "despite intense effort, there is still no atomic-scale picture of the dynamics of this important gas-surface reaction."[6]

The aim of the present theoretical study is to provide greater insight into the mechanism of chemisorption. We have analyzed CH_4 dehydrogenation on a complicated reconstructed surface, Pt{110}-(1×2) (shown in Fig. 1), which closely resembles the rough surface of a metal catalyst. Our calculations feature probably the most precise characterization of the transition states, local minima and pathways to date for such a system, which enables us to comment in detail on the dissociation mechanisms. Our results demonstrate the presence of activated channels for the dissociation process, which are assisted by excitation of both CH_4 stretch and bend modes.

In this work, energies and gradients were calculated using the CASTEP code[9] for supercells with a (2×2) cross section and a six-layer Pt slab to model the Pt{110} surface with the (1×2) missing row reconstruction on one side. The details of these electronic structure calculations are nearly all the same as in previous work,[10,11] except that the kinetic energy cutoff for the plane wave basis was set to 340 eV and the convergence tolerance for the self-consistent-field (SCF) calculations was tightened to 5×10^{-8} eV per atom. Initial guesses for transition state (TS) geometries were obtained using constrained minimization, as in previous work, with a convergence criterion of 0.1 eV/Å for the root-mean-square (RMS) gradient on the CH_4 atoms. Many different surface sites were initially considered (Fig. 1), but we found that CH_4 preferentially dehydrogenates over ridge atop surface sites. The most promising TS candidates were then further optimized by hybrid eigenvector-following methods,[12–14] using the OPTIM program,[13] which has been interfaced to CASTEP. This is a fully unconstrained technique, not previously applied in surface studies. Since analytical second derivatives of the potential energy are not available, variational eigenvector refinement with tangent space minimization was employed.[12–14] The resulting stationary points were converged to an RMS force of 0.003 eV/Å, or better, in each case. This condition corresponds to about 10^{-4} atomic units, which probably represents the highest precision achieved for calculations of this sort to date. We found the corresponding potential energy surface to be rather flat, indicating that tight convergence conditions are essential to properly characterize the mechanisms. For example, structures with an RMS force an order of magnitude greater can have significantly different geometries and energies compared to the true stationary points.

Three of the candidate transition states obtained by constrained geometry optimization eventually produced the same pathway, although the energy decreased by between 0.3 and 1.0 eV on accurate refinement by hybrid eigenvector-following. All three of these pathways are superimposed in Fig. 3, since they provide us with a useful estimate of the precision achieved in these calculations. The corresponding transition state is $[1\bar{1}0]_{TS}$. The other transition state, $[111]_{TS}$, was located only once; the corresponding energetics are summarized in Table I.

For each transition state, steepest-descent paths lead downhill in two directions to the connected local minima. In the present work, approximate steepest-descent paths were

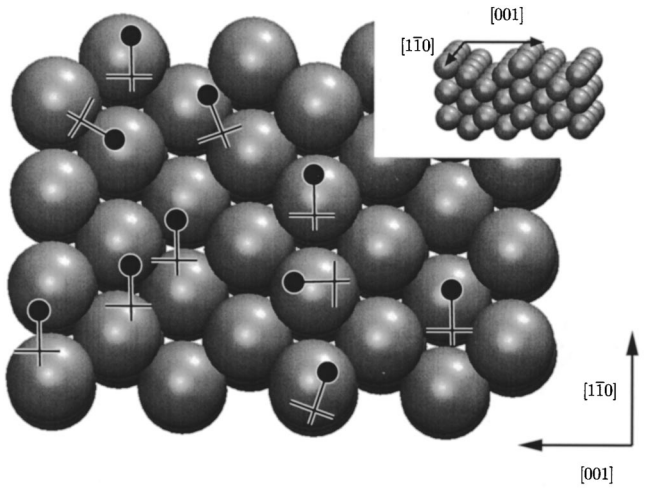

FIG. 1. Dissociation was initially investigated at various Pt{110}-(1×2) surface sites as indicated; CH_4 is shown as a black cross, and the breaking H as a filled black circle. A perspective view of the clean surface is shown in the inset.

TABLE I. Properties of the stationary points located in the pathway calculations. Pt atoms in the top three layers were unconstrained in these calculations. Energies are in eV, and the common energy of the chemisorbed minima (to within the precision of the calculation) was chosen as the arbitrary zero. E_{des} is the energy of the surface plus gas phase methane, E_{TS} is the energy of the TS, and E_{ads} is the energy of the adsorbed state. ΔE_{ads} and ΔE_{des} are the corresponding barriers to adsorption and desorption, respectively. The final column gives the unique negative Hessian eigenvalue at the transition state in eV/Å^2. The energies of the stationary points are converged to a precision of about ±0.01 eV.

	E_{des}	ΔE_{ads}	E_{TS}	ΔE_{des}	E_{ads}	Eigenvalue
$[1\bar{1}0]_{TS}$	0.12	0.40	0.52	0.52	0.00	−5.3
$[111]_{TS}$	0.11	0.40	0.51	0.51	0.00	−3.9

calculated by energy minimization following displacements of 0.02 Å parallel and antiparallel to the transition vector. Here, the transition vector corresponds to the Hessian eigenvector associated with the unique negative Hessian eigenvalue, both of which were obtained using a variational Rayleigh–Ritz approach.[12–14] Energy minimization was achieved using a modified version of Nocedal's LBFGS scheme.[15] For the minima corresponding to gas phase methane the optimization was simply terminated when the required RMS force condition was met. Since the density functional theory employed in the present study does not treat dispersion correctly, we will not speculate about whether physisorbed local minima exist, since this potential would not satisfactorily describe such species. Some authors have attempted to correct for such dispersion effects using additional empirical potentials,[16] but we have chosen not to introduce further parameters into the present calculations. The local minima obtained from the pathway calculations are also described in Table I, and the corresponding pathways are illustrated in Fig. 2. The reaction coordinate for either pathway is found to be a linear combination of both CH_4 stretch and bend modes. All the energy profiles are shown in Fig. 3 and geometrical parameters for the transition states and minima corresponding to chemisorption are shown in Fig. 2.

Upon dissociation, the resulting CH_3 moiety was found to reside preferentially at the ridge atop site. In contrast, the location of the H atom immediately after dissociation depends upon the transition state involved. The two possibilities are the bridge site between two ridge atoms and the

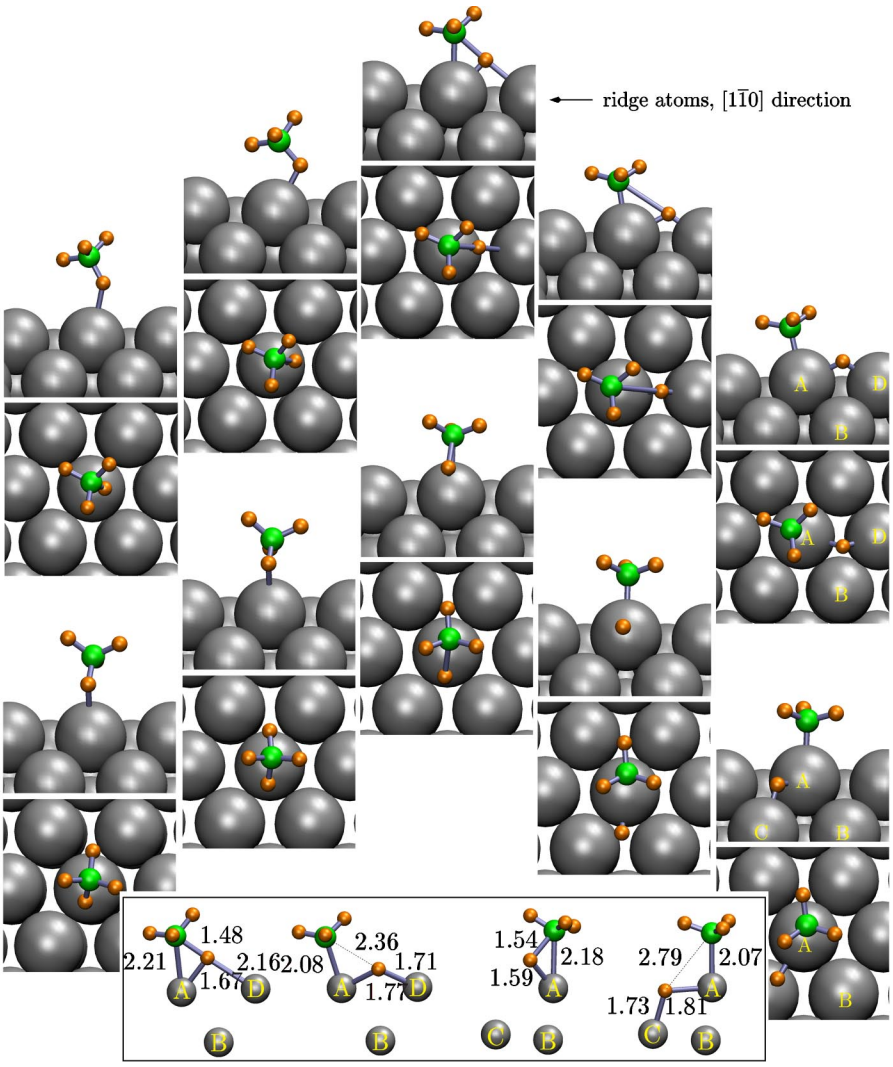

FIG. 2. (Color online) Snapshots of the pathways for $[1\bar{1}0]_{TS}$ (top) and $[111]_{TS}$ (bottom). The left, middle, and right panels correspond to the gas phase methane minimum, the transition state, and the adsorbed minimum, respectively. The other two panels are snapshots of an intermediate geometry along the corresponding path. The vertical displacement of each panel is intended to indicate the relative energy of the corresponding structure. Two views are provided for each path: one from directly above the surface, and the other from a tilted perspective. A cutoff of 2.3 Å was used in drawing the bonds. The inset shows geometrical details of the transition state and chemisorbed minimum for $[1\bar{1}0]_{TS}$ (left pair) and $[111]_{TS}$ (right pair); the distances are in Å.

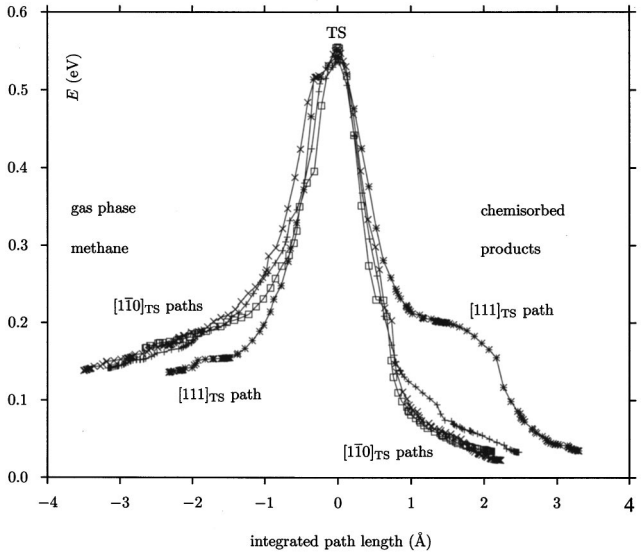

FIG. 3. Energy (eV) as a function of integrated path length (Å) for four paths, three of which correspond to $[1\bar{1}0]_{TS}$ and the other to $[111]_{TS}$ (see also Table I).

bridge site between a ridge atom and a second-layer atom. Ultimately however, the lowest energy closely coadsorbed geometry features the H atom at a second-layer atop site. This structure is 0.25 eV more stable than a gas-phase CH_4 molecule above a clean surface. Several other structures with CH_3 at an atop ridge site and H at other high symmetry surface sites were found to be only marginally less stable, within the 0.1 eV range. CH_3 and H adsorbed in separate (2×2) unit cells is 0.16 eV more stable, suggesting that surface segregation would occur. At moderate temperatures, however, CH_3 will further dissociate yielding either adsorbed methylidine or carbon,[10,11] while hydrogen will desorb.

A model of the interactions at $[1\bar{1}0]_{TS}$ was constructed from a Kohn-Sham one-electron eigenstate analysis. The orbitals of equilibrium and TS-like distorted gas phase CH_4, have been compared with those in $[1\bar{1}0]_{TS}$. The important one-electron Kohn-Sham orbitals are shown in Fig. 4. Distortion of gas phase CH_4 leads to symmetry breaking in the t_2 orbitals; in particular, the component corresponding to the breaking C—H bond (labelled $1t_{2A}$), is strongly destabilised. Mixing of $1t_{2A}$ and $1t_{2C}$ orbitals with each other and with delocalized Pt surface orbitals, occurs in $[1\bar{1}0]_{TS}$. Higher lying antibonding CH_4 states are not believed to be involved

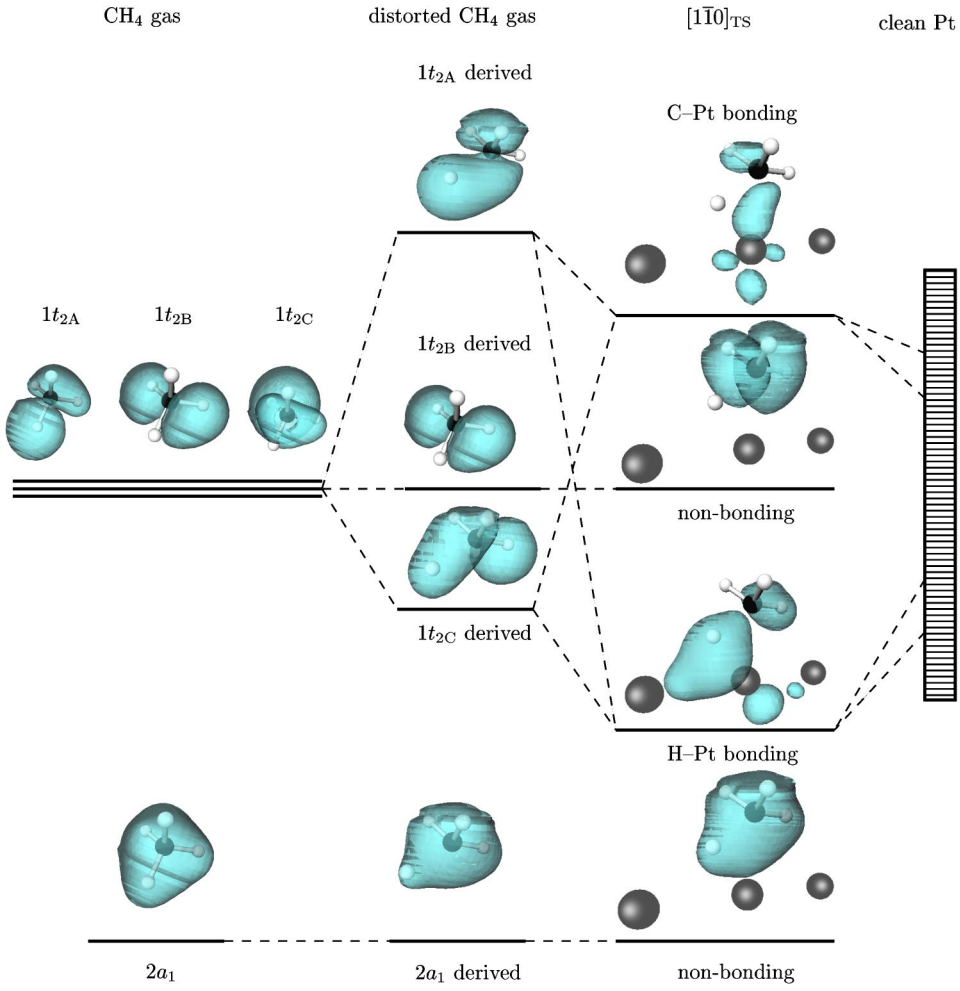

FIG. 4. (Color online) One electron Kohn-Sham real eigenstates.

due to the large energy mismatch with the Pt *d* states.

In summary, two distinct activated pathways were found for dissociative CH_4 chemisorption on the highly corrugated Pt{110}-(1×2) surface. Since our calculations provide a precise reaction coordinate at the TS, unlike previous studies (for example, on Ni{111} by Kratzer *et al.*[17]), we can unambiguously conclude that both stretch and bending modes are involved in dissociation. The present results demonstrate that pathways for dissociation on metal surfaces are considerably more subtle than has, perhaps, been appreciated hitherto. Elucidating the corresponding stationary points and pathways requires precise geometry optimization of the type employed by this study. The commonly used constrained minimization approach, although useful for suggesting transition state candidates, does not provide properly converged structures.

The absence of a barrierless pathway suggests a reinterpretation of experimental data. In their supersonic molecular beam study, Walker and King[3,4] distinguished two different mechanisms for CH_4 dissociative adsorption on Pt{110}: one that yields high dissociation rates as the translational energy is lowered, and another that becomes fast only at high translational energies. The former mechanism was attributed to a steering-assisted process over a negligible barrier, while the latter mechanism was clearly activated. An alternative precursor-mediated explanation for the low translational energy process, in which incoming molecules are trapped into a weakly bound molecular state prior to dissociation, was dismissed because it required a memory of the incoming molecule's vibrational excitation state. The present theoretical results, however, now favor the precursor-mediated low translational energy model, in agreement with the earlier conclusion of Seets *et al.*[2] from a study on Ir{110}, and imply a long lifetime for the vibrationally excited angular deformation mode in the molecule in the physisorbed state. This result also suggests that the lifetime of the stretch mode in this state is short, and that its excitation therefore does not increase the dissociation rate at low translational energies. In the experiments at high translational energies it was concluded that only the stretch mode excitation caused an increase in the dissociation rate. This observation may be due to the experimental method, where the vibrational temperature of the gas was changed, and the mode excited was inferred from an Arrhenius plot. This approach would be biased towards the process with the higher excitation energy. Of course, as the vibrational molecular temperature is raised the excitation of the deformation modes is also increased. State selective studies have recently been undertaken on less corrugated metal surfaces. For example, on Ni{111} Smith and co-workers[8] have compared the dissociative sticking probability for the ground vibrational state and $v=1$ excited asymmetric stretch of CH_4 and found a vibrational enhancement for all translational energies up to 1.45 eV.

The authors gratefully acknowledge support from the Royal Society (S.J.J.) and computer equipment and a studentship from the EPSRC (A.T.A.).

[1] A. C. Luntz and D. S. Bethune, J. Chem. Phys. **90**, 1274 (1989).
[2] D. C. Seets, M. C. Wheeler, and C. B. Mullins, Chem. Phys. Lett. **266**, 431 (1997).
[3] A. V. Walker and D. A. King, Phys. Rev. Lett. **82**, 5156 (1999).
[4] A. V. Walker and D. A. King, J. Chem. Phys. **112**, 4739 (2000).
[5] L. B. F. Juurlink, P. R. McCabe, R. R. Smith, C. L. DiCologero, and A. L. Utz, Phys. Rev. Lett. **83**, 868 (1999).
[6] R. D. Beck, P. Maroni, D. C. Papageorgopoulos, T. T. Dang, M. P. Schmid, and T. R. Rizzo, Science **302**, 98 (2003).
[7] A. C. Luntz, Science **302**, 70 (2003).
[8] R. R. Smith, D. R. Killelea, D. F. DelSesto, and A. L. Utz, Science **304**, 992 (2004).
[9] M. C. Payne, M. P. Teter, D. C. Allan, T. A. Arias, and J. D. Joannopoulos, Rev. Mod. Phys. **64**, 1045 (1992).
[10] M. A. Petersen, S. J. Jenkins, and D. A. King, J. Phys. Chem. B **108**, 5909 (2004).
[11] M. A. Petersen, S. J. Jenkins, and D. A. King, J. Phys. Chem. B **108**, 5920 (2004).
[12] L. J. Munro and D. J. Wales, Phys. Rev. B **59**, 3969 (1999).
[13] D. J. Wales, *Energy Landscapes* (Cambridge University Press, Cambridge, 2003).
[14] Y. Kumeda, L. J. Munro, and D. J. Wales, Chem. Phys. Lett. **341**, 185 (2001).
[15] D. Liu, and J., Nocedal, Math. Program. **45**, 503 (1989).
[16] G. Henkelman and H. Jónsson, J. Chem. Phys. **115**, 9657 (2001).
[17] P. Kratzer, B. Hammer, and J. K. Nørskov, J. Chem. Phys. **105**, 5595 (1996).